4. DISCUSSION

The generation of anti-peptide antibodies by immunization with short synthetic peptides appears to be a frequent event. However, quantitative, comparative studies concerning the antigenicity and immunogenicity of synthetic peptides have only rarely been made. If so, they were mostly restricted to methodological aspects or focused on the peptide antigen itself [11,54,60,67,69,70,77,81,98,143-145,147,148,216-223]. A comparative study on the efficient induction of anti-peptide antibodies was lacking and was therefore attempted here.

An extensive set of commonly used carriers and constructs for peptide-immunization was designed and evaluated with respect to peptide immunogenicity. Sequence motifs of three outer membrane and secreted proteins of the human pathogen *Neisseria meningitidis* were selected as model antigens: Two 20-mer peptides derived from neisserial Opc invasin and serogroup C IgA1-protease, and a 50-mer peptide from serogroup A IgA1-protease. The biological background of these synthetic peptide antigens was illustrated in the introductory part of Chapter 3.2.

The peptide antigens were prepared in 29 different immunogen formulations, including free peptides, liposomal peptide antigens, MAPs, tetra-oximes and 5 different protein-carrier conjugates. Cytokines IL-4 and GM-CSF were tested as adjuvants in three formulations. Peptide-immunogen synthesis and molecular characterization were covered by Chapters 3.2 and 3.3. The peptide constructs were surveyed employing a BALB/c mouse model to evaluate their efficiency on immunogenicity of synthetic peptide antigens.

Intriguing differences in peptide immunogenicity depending on immunogen formulation could be observed and were reported in Chapter 3.5.2. The following Chapters 4.1.1 to 4.1.5 discuss these observations and summarize relevant findings. Considerable emphasis is placed on the discussion of the molecular characteristics of the protein conjugates. Chapter 4.1.4 stresses the impact of molecular context on

carrier immunogenicity such as size, coupling ratio and the intrinsic immunostimulatory potency of the peptide antigens themselves. This peptide/carrier interdependence is the connecting theme to Chapter 4.2 which discusses exceptional structural and immunological characteristics of the peptide 50-mer IgA1-PA50.

Finally, Chapter 4.3 illustrates the pharmaceutical relevance of synthetic peptide antigens and discusses the history and future of synthetic peptide vaccines.

4.1. Effectiveness of different common carriers and immunogen formulations on immunogenicity of synthetic peptides

The immunogens were predominantly associated with a Th2 response.

As seen in Chapter 3.5.2, murine immune reactions were characterized by high frequencies of isotype IgG1-secreting splenocytes (Figure 23 through Figure 25, p. 102 ff.). IgG2a-ASC were not detected or appeared in very low frequencies (data not shown). Antibody isotype IgG1 (along with IgE) is considered as being indicative of a Th2 profile, while high IgG2a levels would signal a Th1 profile [116,116,121,122,126,224]. Thus, an antibody dominated Th2 immune response was induced in all cases.

As outlined in Chapter 1, several parameters influence the type of the immune response, including the route of administration, the dosage, frequency and timing of immunization, the formulation of immunogens and adjuvants, and the type of organism to be investigated.

Here, BALB/c mice were employed as model organism and peptide- or protein-antigens applied. It is known that BALB/c mice favor Th2 responses [125,126,225] one reason for which seems to be their inclination to a comparatively high IL-4 responsiveness [226]. Moreover, Incomplete Freund's Adjuvant was used in injections 2 and 3; it steers the immune response towards Th2 [125] (while CFA applied in injection 1 seems to drive Th1 [126]). One of the protein carriers tested, tetanus toxoid (TT) has also been shown to preferably induce Th2 [142]. Protein- and peptide antigens in general have been demonstrated to preferably induce a Th2 response as well.

4.1.1. Free peptide antigens

Only one out of three peptide immunogens proved immunogenic as "free peptide".

Of the three peptide antigens included in this study, only IgA1-PA50 could stimulate a significant IgG response as "free peptide" under the experimental conditions selected (Pep; Figure 23 through Figure 28, p. 102 *ff*).

4.1.2. Liposomal peptide immunogens

Liposomes did have an immunostimulatory effect only in case the peptide antigen was itself immunogenic.

The two 20 amino acid liposomal antigens (L) of Opc loop 2 and IgA1-PC20 did not show an immunostimulatory effect (Figure 26, p. 106, upper and central panel). In contrast, the immunogenicity of peptide IgA1-PA50 was markedly enhanced with liposomes (Figure 26, p. 106, bottom).

4.1.3. MAPs and tetra-oximes

MAPs did not have an immunostimulatory effect on the peptide 20-mers.

Since the synthesis of MAPs to the IgA1-PA50 50-mer failed, only Opc loop 2 and IgA1-PC20 were tested as multiple antigenic peptides. MAPs did not have a measurable immunostimulatory effect on these peptide antigens (Figure 26, p. 106, upper and central panel).

Tetra-oximes did not have a consistent effect.

Each of the three meningococcal peptide immunogens was tested as a tetra-oxime construct (OX). No immunostimulatory effect could be observed for the 20 aa peptides Opc loop 2 and IgA1-PC20. In contrast, the immunogenicity of the IgA1-PA50 50-mer was markedly increased (Figure 26, p. 106).

The immunogenicity of the tetra oxime-type "synthetic protein" IgA1-PA50 was comparable to ovalbumin and BSA protein-carrier constructs.

The 24.5 kDa Tetra-oxime of peptide IgA1-PA50 was remarkably immunogenic (506 µg/ml peptide specific IgG, OX, Figure 26, p. 106, bottom panel) and was comparable to the "classical" protein-carriers BSA and ovalbumin (691 and 515 µg/ml IgG). It showed a clearly IgG-dominated response and had a better performance than free peptide IgA1-PA50 (Pep) or liposomal preparations (L). Similarly, OX-IgA1-PA50 was OA and BSA comparable at inducing IgG reactive with the parent protein (Figure 28, p. 108, bottom). However, at the cellular level the immunogenicity of OX was less competitive (Figure 25, p. 104): $32/10^6$ peptide specific IgG-secreting spleen cells were counted for OX-IgA1-PA50, versus 61 for BSA and 68 for ovalbumin.

Concluding remarks on Chapters 4.1.1 - 4.1.3

Peptide IgA1-PA50 showed a high intrinsic immunogenicity compared to the two other peptides Opc loop 2 and IgA1-PC20 was the only free peptide antigen able to induce a clear IgM → IgG class-switch (Figure 26 & Figure 27, lower panel, p. 106*f*.). This is indicative for the presence of a T-helper cell epitope in the 50-mer capable of stimulating carrier-independent Th2 responses. Nevertheless, protein carriers did improve the immunogenicity of IgA1-PA50, as discussed below.

Assuming that the superior immunogenicity of IgA1-PA50 is based on the presence of a Th2 epitope, this also implicates that peptides below a certain size may be determined to be poorly immunogenic. The modular integration of both B and T cell epitopes requires a certain peptide size [227]. With respect to Opc loop 2 and IgA1-

PC20, the shorter a peptide, the more unlikely will be a concerted and functional spatial arrangement of B and T cell epitopes on that peptide.

Although non-protein carrier formulations of Opc loop 2- and IgA1-PC20 (Pep, M, OX, L) were not immunogenic, increasing peptide concentration and the number of immunizations might have led to a better response [54].

4.1.4. Protein carrier-conjugated peptides

Protein carrier conjugates were generally immunogenic.

Each of the five protein carrier molecules tested revealed immunostimulatory potency. BSA, KLH, OA, TG and TT invariably induced peptide antigen-specific immune reactions (Figure 23 through Figure 29, p. 102 *ff*).

peptide antigen								
Opc loop 2			IgA1-PC20			IgA1-PA50		
immunogen / carrier	IgG [µg/ml]	MW [kDa]	immunogen / carrier	IgG [µg/ml]	MW [kDa]	immunogen / carrier	IgG [µg/ml]	MW [kDa]
TT	458	193	KLH	2159	3626	KLH	1767	4299
TG	183	330	TG	1758	361	TT	1568	232
KLH	157	3855	TT	1646	187	TG	1546	398
OA	50	50	OA	1170	49	BSA	691	86
BSA	32	77	BSA	492	77	OA	515	51
Pep	0		Pep	0		OX	506	25
CP	0		L	0		COX	226	
L	0		M	0		L	166	n/a
M	0		OX	0		Pep	36	6
OX	0					CP	4	

Table 19: Immunogenicity of different carrier systems and immunogen formulations. Immunogenicity is expressed as concentration of peptide-specific IgG (µg/ml) on day 3 post-immunization. Values represent median values of 5 samples per group of 3 different synthetic peptide antigens Opc loop 2, IgA1-PC20 and IgA1-PA50. Data sorted by descending IgG concentrations.

The influence of size

Size seemed to be beneficial for immunogenicity

As shown in Table 19, there was a marked correlation between size on the one hand and immunogenicity on the other. The three highest ranking carrier systems in terms of induction of peptide-specific IgG (and IgG1-ASC) were also those of maximum molecular weight. The MW of these constructs ranged between 187 kDa and more than 3 MDa. It seems, however, that above a certain molecular weight, size and immunogenicity are no longer strictly correlated. The smallest immunogen of “the big

three", tetanus toxoid, was highly immunogenic and the large KLH immunogens by no means outstripped TT or thyroglobulin. A similar correlation between size and immunogenicity was observed by Houen and co-workers comparing BSA (MW 68 kDa) and PPD (average MW 10 kDa) in which BSA was the more efficient carrier [77].

KLH, thyroglobulin and tetanus toxoid carrier conjugates were significantly more immunogenic than BSA or ovalbumin immunogens.

Regardless of peptide antigen, KLH-, tetanus toxoid- and thyroglobulin-immunogens were significantly more immunogenic than ovalbumin and BSA constructs (Figure 23 through Figure 29, p. 102 ff.). These differences were even more pronounced concerning parent protein cross-reactivity. As visualized in Figure 30, KLH, TT and TG form a distinct group with respect to antigen-specific IgG stimulation. They are contrasted by ovalbumin and BSA conjugates which were characterized by comparatively lower IgG titers.

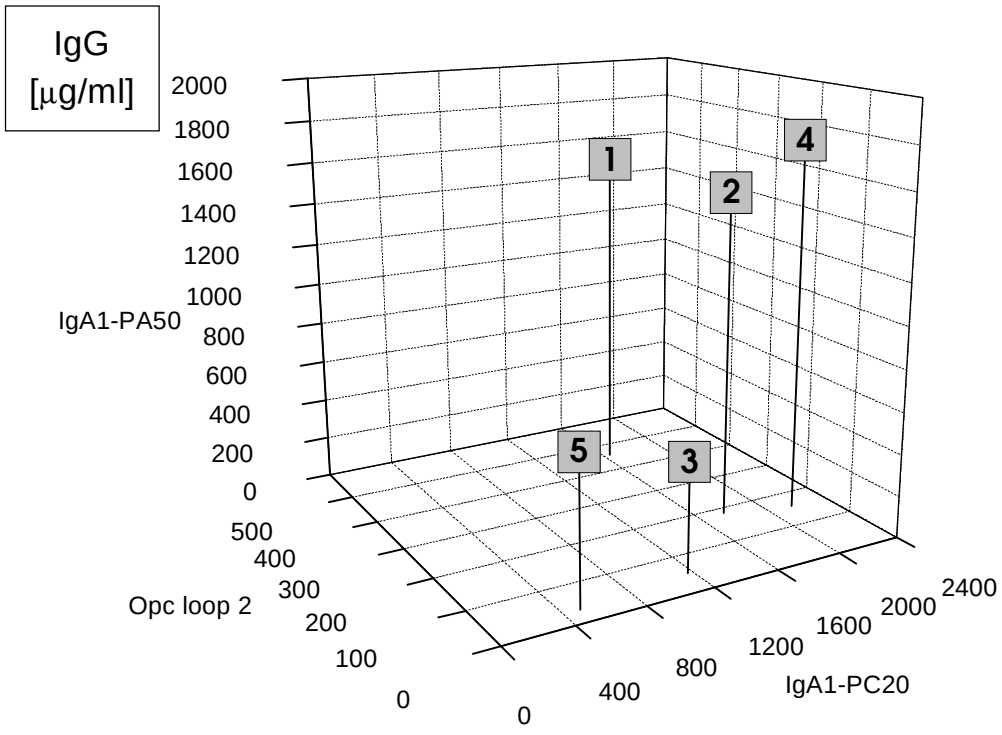

Figure 30: Immunogenicity of tetanus toxoid [1], thyroglobulin [2], ovalbumin [3], KLH [4] and BSA [5] protein carrier immunogens. Data show median serum responses to Opc loop 2, IgA1-PC20 and IgA1-PA50 conjugates in peptide ELISA. Single Factor ANOVA analysis on the protein-carriers showed significant differences within the IgA1-PC20 and IgA1-PA50 carrier subsets: IgA1-PC20: F=5.7, F_c= 2.9; IgA1-PA50: F= 5.9, F_c= 2.9 (F: ANOVA F ratio; F_c: critical F value for rejection at p=0.05 level). No significant differences were seen within the Opc loop2 subset.

These differences were found to be significant for IgA1-PC20 and IgA1-PA50 in Single Factor ANOVA analysis on the peptide-specific IgG response of the protein

carrier subsets BSA, KLH, OA, TG and TT (rejection level p=0.05). No significant differences were seen within the Opc loop2 subset, however.

BSA and ovalbumin are frequently employed as protein carriers for peptide immunization. Both carrier structures are cheap and readily available. Based on the present results, however, these two carriers have a comparatively poor potential to induce an anti-peptide response compared to KLH, TG and TT,.

The influence of coupling ratio

Coupling ratios should be essentially determined by carrier size and the arrangement (frequency) of ε-NH_2 coupling residues on the protein. The size and conformation of the peptide to be conjugated is also of influence. Increasing peptide sizes diminishes coupling efficiency. With increasing size, secondary structure formation may hinder coupling sterically.

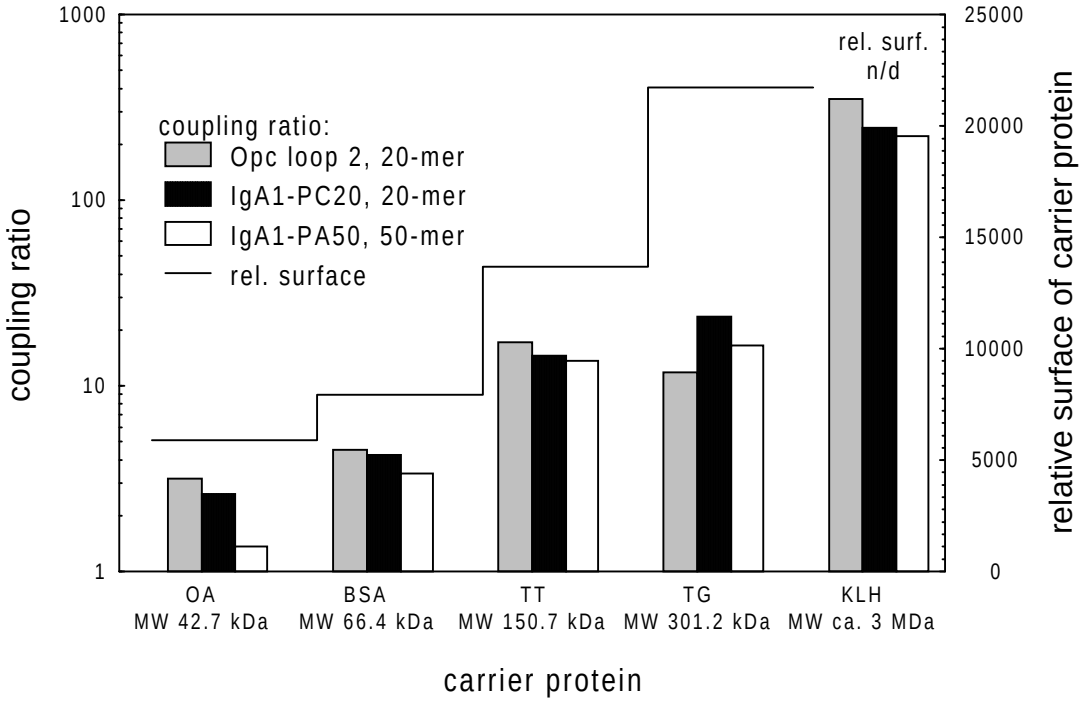

Figure 31: Protein carrier conjugates: *Coupling ratios* to peptide antigens and *relative surface* of carrier proteins. Relative surface was calculated for OA, BSA, TT and TG as described in the text.

As shown in Figure 31, coupling ratios indeed reflected the size and accessibility of the reacting components:

– *The larger the protein carrier, the higher the coupling ratio*: Coupling ratios varied considerably, ranging from as little as 1.4 (OA-IgA1-PA50) for the small ovalbumin carrier to as much as 350 for a KLH conjugate (KLH-Opc loop 2).

– *The larger the peptide ligand, the less efficient the coupling*: Except for TG-Opc loop 2, peptide IgA1-PA50 (white columns) was coupled less efficiently to carriers than peptides Opc loop 2 or IgA1-PC20 (gray and black columns).

KLH, thyroglobulin and tetanus toxoid were characterized by high coupling ratios.

As discussed in the preceding paragraph, the high MW protein carriers KLH, TG and TT formed a distinct group with respect to IgG stimulatory potency. Because of their size, they also share high coupling ratios as a common feature (Figure 31).

A minimum coupling ratio of "1" sufficed for protein conjugate immunogenicity.

It is commonly assumed that 5-20 peptide ligands are sufficient to obtain a good immune response and higher substitution rates may induce unwanted tolerance [228-230]. Here a minimum average of 1.4 molecules IgA1-PA50 coupled to ovalbumin (OA), proved to be effective and was significantly more immunogenic than free peptide (Table 17, p. 90; Figure 26, p. 106).

Carriers	MW, [kDa]	No. of ε-NH_2	Utilization rate ε-NH_2	References
BSA	66.4	59	0.07	[231]
ovalbumin	42.7	20	0.12	[232]
tetanus toxoid	150.7	106	0.14	[233]
KLH [a]	ca. 3000	6.9	n/a	[234]
thyroglobulin	301.2	74	0.23	[235]

Table 20: No. of ε-NH_2 groups of commonly used protein carriers. *Utilization rate* expresses *coupling ratio/No. ofε-NH_2* (Table partly adapted from Ref. [54]; [a] For KLH the number of ε-NH_2 is expressed in g amino acid/100g)

Comparing coupling ratio, ε-NH_2 utilization and surface coupling density.

As seen from Table 20 protein carriers varied considerably with respect to the frequency of ε-NH_2. Note that *No. of ε-NH_2* represents total numbers of ε-NH_2 and not surface exposed residues. Tetanus toxoid is characterized by an exceptional high number of Lys-residues (106). This explained why, despite of being half of the size of thyroglobulin, tetanus toxoid displayed similar coupling ratios as thyroglobulin (Figure 31).

Table 20 lists the frequency of ε-NH_2 residues of the most commonly used protein carriers. Based on the average coupling ratio of the protein conjugates, a utilization rate of ε-NH_2 functions could be determined (Table 20). For BSA, ovalbumin, thyroglobulin and tetanus toxoid between 7 and 23% of the protein carriers' lysine residues were utilized following the protocol in hand. However, there seemed to be no correlation between utilization rate and immunogenicity.

The protein carriers varied greatly in size and coupling ratio. Therefore, the parameter s*urface coupling density* was introduced to provide a less abstract measure for comparing carrier geometry.

Surface coupling density (arbitrary units) calculates the number of coupled peptides to one standardized surface unit. Antigenic peptides are coupled via amino

functions onto the surface of the carrier molecule. With increasing MW the molecular surface does not increase proportionally. Based on the simplistic assumption that the carrier molecules are spherical monomers, carrier volume (i.e. the MW) and carrier surface are related as follows:

(32) $$\frac{V}{A} = \frac{r}{3}; \qquad A_2 = 2 \cdot A_1 \Rightarrow \frac{V_2}{V_1} = 2\sqrt{2}$$

where *V*, *A* and *r* are the volume, surface and radius of a spherical protein carrier.

This means, in order to double the molecular surface ($A_2 = 2 \times A_1$) the MW has to increase by a factor of 2.828, or 3-fold. *Surface coupling density* allows direct comparison of the various protein conjugates. It expresses coupling efficiency based on the potential coupling area instead of the MW. *Relative surface* (arbitrary units, Figure 31), was directly derived from molecular weight, substituting volume by MW. KLH was excluded from this comparative calculation because of its molecular heterogeneity.

Now, *surface coupling density* showed a more homogenous picture of the protein conjugates (Table 21). While the *coupling ratio* varied from 2.4 to 272.8 (a factor of 115) the coupling density indicates that 0.40 to 1.11 peptides were coupled per standardized surface unit (a 2.8-fold range). Antibodies are polyvalently binding to their epitopes and parameters like binding affinity, on-rate and persistence of binding are influencing the immune response. Notably tetanus toxoid, half of the size of thyroglobulin and 1/20 of KLH, was highly suitable as a carrier and showed a comparatively high average coupling density of 1.11.

	protein carrier				
	BSA	KLH	OA	TG	TT
MW carrier, kDa	66	3000	43	301	151
coupling ratio, average	4,0	272,8	2,4	17,3	15,2
surface coupling density, average	0,51	n/a	0,40	0,80	1,11

Table 21: Comparison of protein carrier immunogens. Average coupling ratios and surface coupling densities of BSA, KLH, ovalbumin, thyroglobulin and tetanus toxoid conjugates.

Peptide/carrier-interdependence

Opc loop 2 and IgA1-PC20 immunogens clustered into two groups with respect to immune response intensity: Protein and non-protein carrier immunogens.

Both, ELISPOT and ELISA results provided a picture of striking difference between protein carrier and non-protein carrier formulations of the two 20 amino acid antigens Opc loop 2 and IgA1-PC20. High IgG titers and ASC frequencies of BSA-, KLH-, ovalbumin-, tetanus toxoid- and thyroglobulin-conjugates were contrasted by low titers and frequencies if antigenic peptides were applied as free peptide, MAPs, tetra-oximes or liposomal formulations (Figure 23, p. 102; Figure 26, p. 106). This probably reflects the existence of T cell epitopes on the protein carriers.

As already discussed in Chapters 4.1.1 to 4.1.3, a completely different situation was found with the 50 amino acid IgA1-PA50. Here, also preparations void of protein carriers proved immunogenic (Figure 25, p. 104 & Figure 26, p. 106).

Protein carrier immunogens show higher parent protein cross-reactivity.

Comparing parent protein cross-reactivity for protein and non-protein constructs, there seemed to be a superiority of protein carrier constructs (Table 22, IgA1-PA50). A protein surface represents a very heterogeneous coupling environment. Peptide ligands attached to this surface, may assume multiple conformations that induce antibodies with higher parent protein cross-reactivity than can a free random coil polypeptide. However, the two tetrameric oxime preparations (OX, COX) did show higher cross-reactivity ratios than any of the other non-protein carrier formulations (Pep, CP, L). This observation may reflect a higher degree of ordered structure in OX-/COX-IgA1-PA50. This possibility is discussed in more detail at the end of Chapter 4.2.

No clear conclusions on this topic can be found in the literature. Two comparative studies on MAP induced antibodies observed only limited cross-reactivity with the parent protein in one case [236] but found MAPs to be superior to protein carrier conjugated peptides in a second [147].

IgA1-PC20				IgA1-PA50			
immunogen / carrier	IgG to peptide [µg/ml]	IgG to protein [µg/ml]	ratio	immunogen / carrier	IgG to peptide [µg/ml]	IgG to protein [µg/ml]	ratio
KLH	2159	1702	0.79	OA	515	404	0.78
TG	1758	839	0.48	TT	1568	990	0.63
BSA	491	208	0.42	BSA	691	404	0.58
TT	1645	582	0.35	TG	1546	873	0.56
OA	1170	272	0.23	OX	506	239	0.47
				KLH	1766	777	0.44
				COX	226	88	0.39
				L	166	51	0.31
				CP	4	1	0.25
				Pep	36	5	0.14

Table 22: Cross-reactivity of peptide induced IgG to the parent protein IgA1-protease. Data show IgG serum responses to the two peptide antigens, IgA1-PC20 (20-mer of serogroup C protease) and IgA1-PA50 (50-mer, serogroup A) and the corresponding parent proteins. Concentrations are expressed as median of antigen-specific IgG (µg/ml) 5 serum samples per group as determined in peptide and protein ELISA. Cross-reactivity "ratio" = IgG α-protein/IgG α-peptide. Data sorted by descending ratio.

IgA1-PA50 conjugates induced higher antibody affinity to the cognate parent protein than IgA1-PC20 conjugates.

Notable differences were seen between the 20 amino acid peptide IgA1-PC20 and the 50 amino acid peptide IgA1-PA50 regarding cross-reactivity with the parent protein. Both peptides are derived from the same region of two IgA1-protease variants. IgA1-PC20 encodes 20 amino acids of serogroup C and IgA1-PA50 50 aa of serogroup A

protease, with the latter overlapping the 20-mer on both sides. In the parent protein framework they are both surface exposed and proven to be recognized by α-protease serum antibodies [150]. While both peptides stimulated comparable IgG responses to the immunizing synthetic peptide antigen, a higher proportion of IgG directed against IgA1-PA50 also recognized the parent protein. Except for KLH, the α-IgA1-PA50 responses showed 16 to 55% higher ratios of IgG cross-reacting with the parent protein (Table 22).

Opc loop 2 and IgA1-PC20 had different carrier preferences.

Judging from IgG titers and IgG-ASC frequency (Table 19, Figure 23 + Figure 24) the two 20 aa peptides Opc loop 2 and IgA1-PC20 induced maximum IgG titers and ASC frequencies with different protein carriers. Opc loop 2 worked best conjugated to tetanus toxoid while IgA1-PC20 was most immunogenic when coupled to KLH. This peptide/carrier interdependence suggests that different carriers may be preferable for different peptides.

One question that was not answered with the present experimental set-up was the immunogenicity in a primary response regime, i.e. the potency of raising an immune response after a single challenge, or in the absence of adjuvants.

Concentration effects

Protein carrier KLH, highly immunogenic by itself, did not induce immunological paralysis as described elsewhere [70,102,237]. It remains unclear whether immunological paralysis is due to a dose response phenomenon. Kanda and colleagues for instance, injected as much as 30 µg KLH conjugate per mouse in contrast to 2.2 - 3.9 µg in this study, where all three KLH constructs were highly immunogenic.

Both protein carrier and non-protein immunogens were tested as part of this study. Due to the molar normalization of the peptide antigens to 200 pmol/injection, immunogen preparations varied considerably in protein concentrations (Table 18, p. 91). Concentrations ranged from 0 µg protein/injection for the non-protein carrier constructs to 7.4 µg protein/inj. for IgA1-PA50 coupled to ovalbumin. It is unclear to what extent protein concentration effects contributed to response differences and a dose response study would be required to elucidate dosage effects.

4.1.5. Cytokines as adjuvants

Cytokines as adjuvants had contradictory effects.

Cytokines IL-4 and GM-CSF were co-administered as adjuvants with peptides Opc loop 2 and IgA1-PA50 and with the IgA1-PA50 tetra-oximes. These adjuvants had effects both on serum titers and ASC frequencies.

Free peptide Opc loop 2: Cytokines resulted in a small elevation of IgM serum titers and numbers of IgM antibody-secreting cells (Figure 23, p. 102 & Figure 26, p. 106).

Free peptide IgA1-PA50: Contradictory responses in spleen and serum were observed: Peptide antigen-specific ASC (IgM and IgG1) and IgM serum titer

increased, but IgG titers diminished compared to the cytokine-free formulations (Figure 25, p. 104 & Figure 26, p. 106).

Tetra-oxime IgA1-PA50: Both IgG1- and IgM-ASC frequencies increased while IgG titers went down (OX, COX).

In order to interpret these seemingly conflicting observations it is noteworthy that the information provided by ELISA and ELISPOT is essentially different. ELISPOT counts cell numbers, ELISA estimates antibody titers. ELISA provides systemic information (because antibodies are circulating in the blood stream) while splenocyte analysis (ELISPOT).

Injection No. 2 and 3 were prepared in Freund's incomplete adjuvant (IFA) and applied intraperitoneally. IFA limits dispersion and retards the release of the immunogen preparation. If cytokines had a predominantly local effect, the spleen would have been the most proximal lymphatic organ to the i.p. injection site. A "localized effect" of the cytokines would explain the increased frequency of antigen-specific splenocytes and the impression that this increase does not break through to the serum level. It would not explain, however, why ELISA IgG-titers contrarily diminished.

The spleen is not the sole site where antibody-secreting cells can be found, however. B-lymphocytes are circulating entities which can also be isolated as circulating peripheral blood mononuclear cells, and there are other more distal "hot spots" of B-cell presence such as lymph nodes, bone marrow, tonsils or Payer's patches. While only B-lymphocytes derived from spleen were analyzed in ELISPOT the entirety of antibody-secreting cells contributes to the antibody titers measured in ELISA.

One possible explanation for these diametrical effects is that the administration of IL-4 leads to an imbalance of other cytokines *in vivo* and that this has contradictory effects on antigen-specific and polyclonal responses. In a study by Van Ommen *et al.*, the *in vivo* administration of IL-4 caused an increase in the levels of non-specific polyclonal IgG1 and IgE, but a marked decrease in the levels of antigen-specific IgG1/IgE and the formation of memory B-cells [238].

Concluding remarks on Chapter 4.1.5

The two tested cytokines IL-4 and GM-CSF showed relatively minor or counterproductive effects on peptide immunogenicity and do not justify adding these substances to immunogenic formulations under the conditions investigated.

4.2. Structural and immunological characterization of peptide IgA1-PA50

Among the three synthetic peptide antigens included in this study, IgA1-PA50 proved significantly more immunogenic than peptides IgA1-PC20 and Opc loop 2. Due to this intrinsic immunostimulatory potency, the integration of peptide IgA1-PA50 into non-protein immunogens, such as liposomes and tetra-oximes, resulted in enhanced immunogenicity of these constructs. Therefore, it seemed worthwhile to take a closer look on this peptide antigen, namely its structure and immunological determinants.

In the following chapter, structural insights gained on IgA1-PA50 by CD analysis are compared to NMR-data. Subsequently, results obtained on the immunogenicity of the peptide (*Immunogenicity Study*, Chapter 3.5.2) are contrasted with data of a MHC class II binding motif analysis and the structural and immunological characteristics of peptide IgA1-PA50 are discussed. Figure 33 (p. 127) concludes this chapter providing a graphical compilation of the data.

CD spectroscopic studies

CD measurements have been extensively used to estimate secondary structures in peptides [107,164,239-244]. CD-spectral data indicate a high propensity for secondary structure in IgA1-PA50.

The CD spectrum of IgA1-PA50 is characterized by a positive maximum at the 186 nm band and a negative maximum at the 198 nm band (Figure 14). The spectrum mainly resembles an antiparallel β-sheet reference spectrum [245,246]. However, the positive maximum and the intense negative band are both located at comparatively short wavelengths (λ=186/198nm). This blueshift can be explained by the contribution of random coil and β-turn stretches [188,247,248]. These initial impressions are supported the following analysis.

CD-spectrum deconvoluted data

Although varying results were calculated depending on the method, secondary structure estimation revealed β-sheets and β-turns as the predominant structural elements (Table 15 & Table 16).

Variable Selection [164] and *CONTIN* [163] disagreed in estimating helical conformations (7%/0% respectively). Both regarded β-structures as major structural elements of IgA1-PA50 (β-sheet 35%/52%, β-turn 21/15%). As for the α-helical contents, the estimation by VS seems to be more reliable since CONTIN is restricted to λ≥190 nm, thus neglecting information provided by the positive band at λ=186 nm for iteration. Both methods are in high agreement for the estimation of remainder structures (35%/33%).

Spectrum comparison with the spectral library of the Variable Selection data set identified the CD-spectrum of elastase (Figure 32) as coming closest to that of IgA1-PA50 (Figure 32, small inset). Both spectra are characterized by a positive maximum below 190 nm and a negative maximum below 200 nm which is combined with a negative shoulder in the peptide bond region (190 nm ≤ λ ≤ 240 nm). This is also reflected in the correspondence of the secondary structure contents (Table 23).

α-helix	β-sheet		β-turn	remainder	Σ	
	parallel	anti parallel				
IgA1-PA50						
0,07	0,01	0,34	0,21	0,35	0,98	VS
0,00			0,15	0,33	1,00	CONTIN
Elastase						
0,10	0,00	0,37	0,22	0,31	1,00	

Table 23: Comparison of secondary structure contents of synthetic peptide IgA1-PA50 to elastase. Secondary structure estimates are derived from CD (IgA1-PA50, this work) and X-ray analysis (elastase, [164])

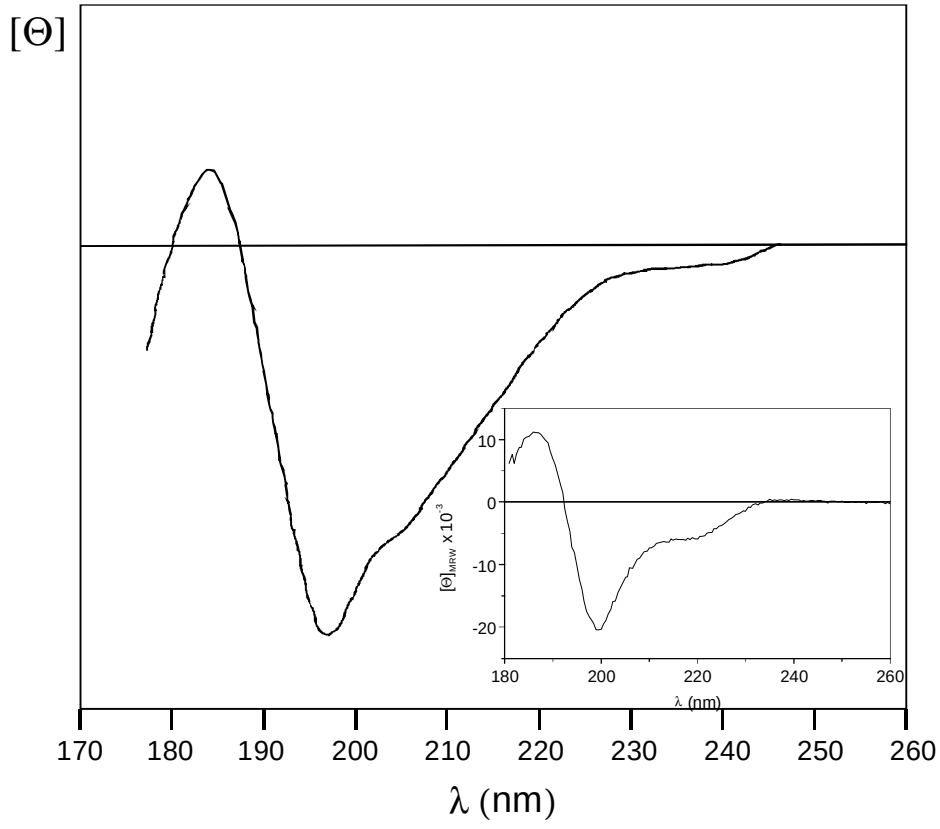

Figure 32: CD spectra of elastase (Spectrum reproduced from the Variable Selection package [164]) and of synthetic peptide IgA1-PA50 (small inset).

The cross-reactivity of MAb AH623 between cognate IgA1-protease and peptide IgA1-PA50 stimulates the question to what extent the secondary structure of IgA1-PA50 mimics epitope 4 within the native protein framework. No structural data on IgA1-protease are available, however.

The same question, whether the peptide's solution structure in CD resembles the parent protein structure, was investigated by Bhattacharjya *et al.* on riboflavin. They found good agreement between crystal structure data of the native protein and the NMR and CD nascent structure analysis of protein derived synthetic peptides [249]. Yang *et al.* retrieved identical CD-spectra for both the native hen lysozyme and a mixture of 4 dissected peptides spanning the protein sequence [250]. Hamada *et al.* made contradictory observations: peptide fragments of the β-sheet protein β-lactoglobulin had helical propensities in solution [251].

Sequence based structure prediction

Sequence based structure predictions by the methods of Chou-Fasman [161] and Garnier-Osguthorpe-Robson [252] showed that predictions for the "remainder" structures were in excellent agreement with CD analysis derived calculations. Less agreement is seen in comparing β-turns: The predictions deviated 3-17% from the CD estimates. High disagreement is seen among the estimates and predictions for β-sheet and α-helix elements: α-helix contents is overestimated, β-sheet underestimated. It is noteworthy that both methods were originally developed for secondary structure prediction of globular proteins and tend to overestimate α-helix formation in synthetic peptides [253].

However, the fact that α-helix formation could not be seen in CD does not render sequence based predictions inapplicable. A given dynamic peptide structure with the intrinsic propensity for secondary structure formation -say an α-helix- may stabilize this latent helix upon antibody binding. Indeed, it has been shown that interactions with the antibody binding site can promote helix folding of shorter peptides [254,255]. Dyson *et al.* created the term *nascent helix* for the adoption of a transient helical structure in aqueous solution which is stabilized in TFE [256,257]. Gras-Masse *et al.* suggested a "dynamic equilibrium" for peptides with intrinsic conformation that are too small to exhibit a lasting secondary/tertiary structure [258]. Regions of peptide immunogens that contain conformational preferences for ordered or nascent secondary structure have been implicated in the mechanism of induction of anti-peptide antibodies [257,259-269].

A graphical representation of the sequence based structure prediction results is displayed Figure 33, p. 127, lines *5-10*. Both methods locate α-helical stretches in the C-terminal region of the peptide. Hence the dominant structural elements of the peptide seem to be β-sheets and -turns at the N-terminus, and possibly a "nascent" α-helical stretch at the C-terminus. The N-terminal β-strand region is "fenced in" by a typical β-strand breaking amino acid, glycine, at gly^{14} and gly^{15} [270].

Buffer and concentration effects on peptide conformation

Varying solvent environments did not change secondary structure: Uniform CD-spectra of Iga1-PA50 were obtained for the three solvent environments H_2O, 10 mM

Na-phosphate pH 4.5 and 10 mM Na-phosphate 7.0 (Figure 14, p. 86). The spectrum changed slightly with increasing peptide concentrations. Although the peak ellipticities at λ=186 nm and λ=198 nm decreased, the methods of Manavalan and Johnson or Provencher and Glöckner did not calculate a qualitative change in secondary structure contents.

Thermal stability of the peptide

After melting the molecule at 80°C IgA1-PA50 100% reversibly regained its original spectrum, i. e. its structure. This striking observation indicates a well organized and "conservative" solution structure of the peptide.

Following the temperature effect on the 222 nm band, the melting curve expresses a sigmoidal shape (Figure 15, p. 88). The thermal stability midpoint T_m at 50% fractional change was determined to be 53°C. Hence, the thermal stability is comparatively high [271]: Nomizu *et al.* analyzed laminin peptide derivatives of high helix propensity. They found T_ms ranging from 39 to 51°C for peptides of 63, 82 and 105 aa in length that formed coiled-coil dimers in some cases. Only one triple-stranded coiled-coil dimer of 105+55 amino acids showed a higher T_m (T_m=62°C) [271]. An immunogenic cyclized octadecapeptide analyzed by Lamthan *et al.* showed T_ms of 32°C and 44°C depending on the buffer environment [261]. Benchmarks for exceptionally stable synthetic peptides are provided by the work of Monera *et al.* Their *de novo* design of coiled-coil model peptides (70-mers) resulted in molecules with T_ms between 56°C and 75°C [272].

NMR data

Peptide IgA1-PA50 was also analyzed by NMR. This work was carried out by our colleagues Jeremy Derrick and Lu Yun Lian at Manchester University (data not shown). 1-D ^{1}H, 2-D TOCSY and NOESY NMR were carried out in H_2O and D_2O.

These results confirmed some of the CD analysis and sequence based computational structure predictions [273]. The molecule did not show an α-helical conformation and appeared to be composed of beta strand and random coil. Assignments were found for L1 through Y6, Y8 through A10, G14 through S16, Q26 and T27 and D31 through M35. All residues in each of these stretches are connected via $C_\alpha H(i)$ to NH(i+1) NOEs (i.e. α-carbon protons were seen in close vicinity to successive amide protons). This is indicative of an extended beta conformation. Furthermore long range NOEs unveiled non-local amino acid interactions demonstrating strong circumstantial evidence for a regular tertiary structure. However, these long range NOEs could not be reliably assigned.

The overall picture seemed to be a loosely folded protein of 4 (to 5) beta strands that are associated together with a hydrophobic core, comprising W32 and several of the tyrosine residues at the N terminus. Branching out from the end of these strands are the loops which appear highly mobile [273]. In Figure 33 (p. 127, line *2*) the beta strands are indicated by "**b**" and the interactions of W32 with the N-terminal tyrosines to form the hydrophobic core are symbolized by a connecting line; the unassigned stretches V17 to G25 and G36 to K50 would then correspond to the loops. Globular structures with no helix or disulphide bridges of 50 residue or less are extremely rare. It is likely that this core is interacting with the C-terminus as well since binding of the

monoclonal antibody AH 623 binding involves residues at both the N- and C-terminal end of the 50-mer (see below). The C-terminus could also serve as a structural scaffold; in this case C-terminal residues would contribute to AH 623 binding indirectly. However, ELISA is a solid phase type binding assay and thus may differ from NMR results which render solution conformation in absence of antibody. For a more detailed NMR analysis it is necessary to switch to ^{15}N NMR.

Now, rather than random coil, *random meander* would be a better description for the "remainder" structures observed for IgA1-PA50 in CD. A *random coil* is an unfolded polypeptide continuously changing its structure by rotation around its various covalent bonds. The term *random meander* was created by Kyte and characterizes the structural appearance assumed by the backbone of a folded polypeptide that is neither an α-helix, a β-structure, nor a β-turn [274].

The observed structural organization of peptide IgA1-PA50 matches well with the observation that peptide IgA1-PA50 is recognized as a "conformational epitope". MAb AH623, which is reactive with the murine epitope 4 of serogroup A IgA1-protease, binds to the peptide provided that a critical length is exceeded. Increasing length augments binding (data not shown) and N- or C-terminally truncated versions of IgA1-PA50 lose reactivity [275] (Figure 33, p. 127, lines *3* and *4*): Peptide *3* is a 66-mer truncated before Y8; peptide *4* is a 75-mer truncated C-terminally at K43 and prolonged N-terminally. Thus, the minimum length for binding AH623 exceeds 36 amino acids (Y8 to K43).

In case of a continuous epitope, the CDR (complementarity determining region) of an antibody is believed to interact with a maximum of 5 to 8 amino acids of the antigen or 700 $Å^2$ [276-279]. Here the peptidic binding residues must be spatially separated into at least two binding moieties directly (in terms of binding) or indirectly (in terms of structural assistance) involving either end of a minimum length of more than 36 amino acids. Residues participating in binding may even be more dispersed and scatter over the whole peptide.

Definitive information on IgA1-PA50/AH623 interaction requires X-ray data of a crystallized antibody/peptide complex.

MHC class II binding motifs and secondary structure

The suspected existence of a MHC II binding motif on peptide IgA1-PA50 was due to four observations:

1. Peptide IgA1-PA50 was immunogenic by itself (Figure 25, p. 104 & Figure 26, p. 106). In fact, it was significantly more immunogenic than even larger constructs of 4 x 20 aa (MAP, tetra-oxime) of the IgA1-PC20 variant.
2. The responses to the non-protein carrier immunogens of IgA1-PA50 were IgG dominated. This IgM → IgG class-switch requires T cell assistance, hence a T cell epitope (Figure 26, p. 106 & Figure 27, p. 107).
3. In ELISA the synthetic tetra-oxime of IgA1-PA50 is as highly immunogenic as IgA1-PA50 coupled to ovalbumin and BSA (Figure 26, p. 106).
4. A 104 amino acids prolonged version of peptide IgA1-PA50 has been successfully tested as a carrier itself and shown to improve immunogenicity of bacterial capsular polysaccharide [182].

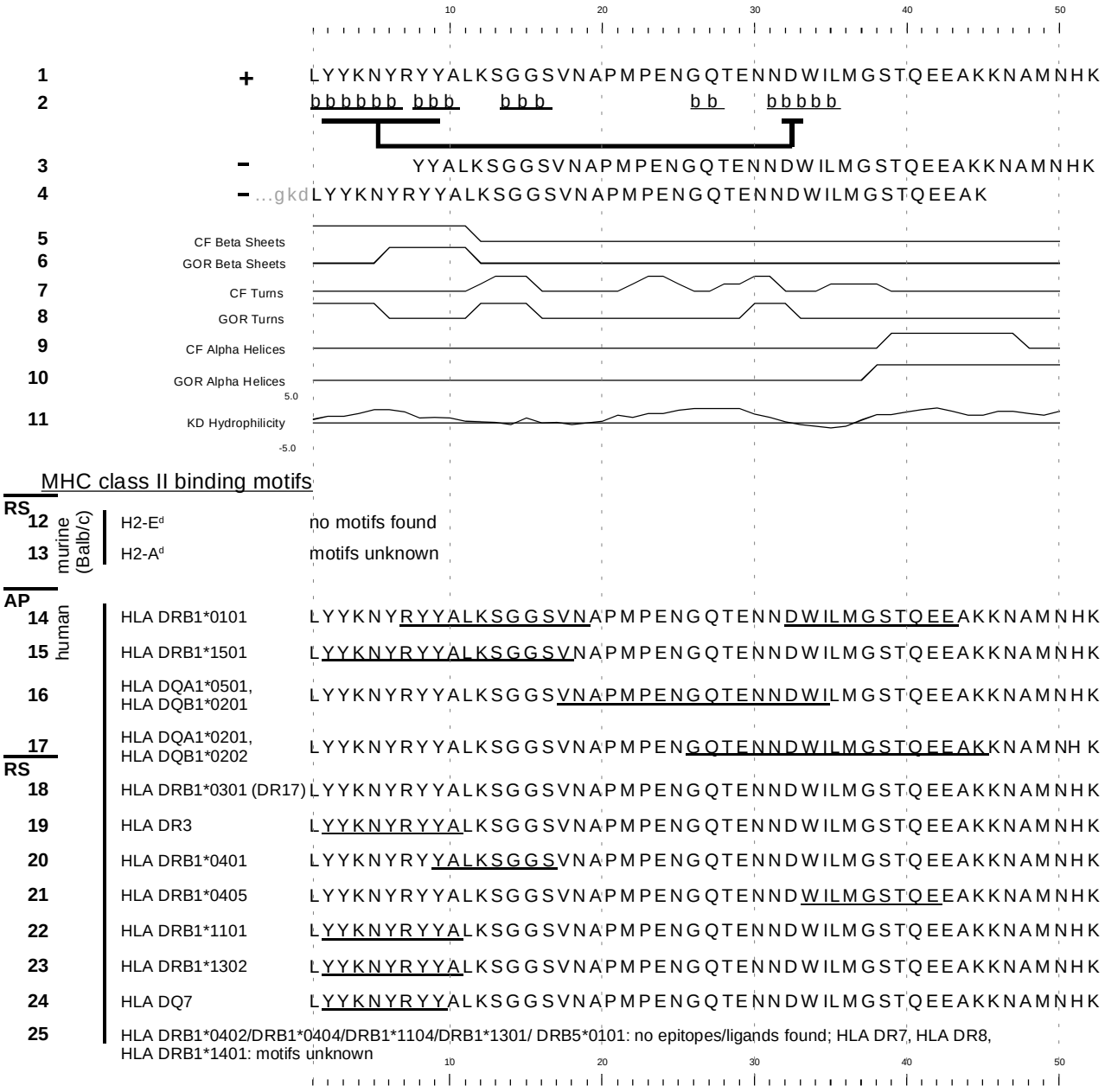

Figure 33: Structural and immunological characterization of peptide IgA1-PA50 (line *1*). AH623 MAb binding: In lines *1*, *3* and *4* peptides of various lengths spanning epitope 4 of neisserial serogroup A IgA1-protease are depicted including the 50 amino acid IgA1-PA50 (line *1*). "+" indicates ELISA reactivity of IgA1-PA50 with the "conformational" monoclonal antibody AH623. N- or C-terminally truncated peptides lose reactivity with AH 623 (-) (lines *3*, *4*) [182,275]. The peptide in line *4* is truncated at K43 but is prolonged N-terminally by 32 aa which is symbolized by a gray-shaded "…gkd" extension. NMR [273]: NMR results on IgA1-PA50 are summarized in line *2*. The observed β-strands are indicated by "**b**" and the interaction of W32 with the N-terminal tyrosines is symbolized by a connecting line. Sequence based secondary structure prediction: Lines *5* to *10* are graphical representations of computational structure predictions for β-sheets, -turns and α-helices based on the methods of Chou-Fasman (CF)[161] and Garnier-Osguthorpe-Robson (GOF)[162]. Hydrophilicity according to Kyte-Doolittle (KD) [280]. MHC class II epitope prediction [38]: MHC class II epitopes/ligands were predicted based on *ACTIPAT* analysis [281] (**AP**, lines *14-17*) or the Rammensee database on class II MHC at Tübingen University (http://www.uni-tuebingen.de/uni/kxi/class2.htm) for murine BALB/c (**RS**, lines *12*, *13*) and human MHC class II binding motifs (**RS**, lines *14-25*).

T cell epitope analysis was kindly carried out by B. Fleckenstein, Tübingen University, based on a new approach for the prediction of T cell epitopes [6,281,282].

In Figure 33 T cell prediction results are summarized. Lines *14-17* are based on a computational approach calculating allele-specific *Activity Patterns* (ACTIPAT) [281]. These data are based on a systematic approach which utilizes a combinatorial undecapeptide library with 2.048 x 10^{14} sequences for screening against known MHC II molecules. Until now, only data on the most frequent human class II MHCs are available. The 21 alleles of human class II MHC investigated (line *14* ff.) approximately cover 95% of a randomized human (Caucasian) population.

In lines *12*, *13* and *18-25* epitopes were predicted based on an epitope retrieval using the SYFPEITHI database on MHC II epitopes at Tübingen University (http://www.uni-tuebingen.de/uni/kxi/). This database represents a collection of empirical data of various authors, from which T cell binding motifs were abstracted. Predicted epitopes or ligands are underlined.

The predicted 9 to 11 amino acid stretches represent core regions of epitopes which are 12-20 amino acids in length.

For none of the two BALB/c MHC II alleles (H2-A^d, H2-E^d) evidence could be found for a murine BALB/c T cell epitope or ligand on IgA1-PA50. This is not surprising since data available on BALB/c T cell epitopes are extremely poor [38]. For the H2-E^d allele (line *12*) only few binding motifs are known. Moreover, these are highly degenerate and it is therefore impossible to positively cover all their potential variants [38]. For H2-A^d, binding motifs could not be deduced at all until now (line *13*).

The notion that there is a Th-epitope on IgA1-PA50 remains speculative and is solely deduced from the four observations above. The following amino acid motifs could come into question for a putative murine T cell epitope [38]: i) the hydrophobic region around I33 and ii) the N-terminal tyrosine cluster extending to the sheet-breaking and turn-inducing double G at G_{15}/G_{16}. These stretches both bear T cell epitopes in human MHC II prediction (Figure 33, lines *13, 15, 19, 20, 22-24* and *14, 17, 21*)

Concluding remarks on Chapter 4.2

The innate tendency to adopt a folded conformation either in solution, or in the bound state with antibodies and B cell receptors is correlated with antigenicity. One prerequisite for stable solution conformation is size. Well defined conformational states have been demonstrated for a wide variety of antigenic peptides in solution [256,283]. Most functional antibodies recognize conformational epitopes [254]. Induction and stabilization of secondary structure in synthetic peptides and the presence of proper T cell epitopes can greatly enhance immunogenicity [107,284].

The highly immunogenic peptide IgA1-PA50 might be useful as a model compound for illustrating principles of peptide immunogenicity:

Size: The 50-mer peptide IgA1-PA50 is larger than the two 20 amino acid antigens Opc loop 2 and IgA1-PC20 and larger than the majority of common synthetic peptide antigens of sizes between 20 and 30 amino acids [54]. However,

even larger synthetic peptide constructs of 4 x 20 = 80 amino acids that were included in this study that were poorly immunogenic (MAPs and tetra oximes of Opc loop 2 and IgA1-PC20).

T cell epitopes: it is likely that one or more MHC II T cell epitopes are located on the peptide.

Structure: Peptide IgA1-PA50 carries a B cell epitope, probably as a conformational epitope cross-reactive with a discontinuous epitope in the parent protein framework. The high secondary structure propensity of IgA1-PA50 is likely to be stabilized and enhanced upon assembly into a tetra-oxime type 24.5 kDa "synthetic protein" leading to enhanced immunogenicity of this compound. Figure 34 gives an example of the structural enhancement of a model peptide forming α-helices due to template attachment. The constraints of the IgA1-PA50 peptide within the tetra-oxime environment may induce conformations favoring antibody recognition. As a tetravalent structure, the oxime-construct also enables multiple binding. Kanda and co-workers described similar phenomena and found that new structural epitopes were created upon peptide multimerization of a 19-mer on an octameric MAP [70]. It would be interesting to substantiate this hypothesis by further CD/NMR analysis.

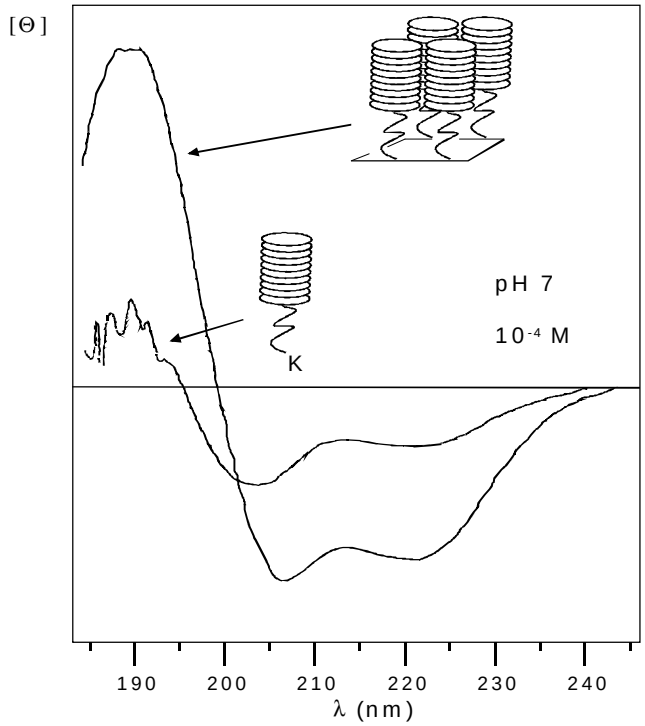

Figure 34: CD spectra of a model peptide with propensity to form helices. Upon attachment to the template, structural contents are increased (Figure adapted from [11]).

4.3. On the history and future of synthetic peptide vaccines

Synthetic peptide vaccines are an appealing concept. The idea to utilize only parts of a pathogen for immunization, thus focusing the immune response to the essential structural and physiological features which determine virulence is obvious. A strong concentrated response interfering with the pathogen's capability to infect is favorable over a broad non-specific immune reaction, for two reasons, namely the specificity of the immune reaction and the decreased risk of autoimmune reactions.

Inducing an immune response to a complex cellular structure, such as an attenuated pathogen, may have undesired side-effects. Immunologic capacity is dislocated. That is low affinity B-cell clones or clones directed to less important structures of the invading pathogen may be expanded by chance at the cost of high specificity variants. Immune exhaustion might be observed as a consequence: In case of the HIV virus, too many hypervariable antigens are presented by a steadily diversifying virus population. The immune response is driven away from the essential virulence factors. Moreover, the induction of a specific immune reaction seems to improve immune response kinetics, speeding up clearance or increasing survival rate [285]. Thus, restricting the challenge to certain key molecules should do the same job more efficiently. Moreover, the risk that potentially autoreactive lymphocytes are activated is minimized.

Advantages of synthetic vaccines over conventional formulations are:

chemical purity
defined structure/contents
exclusion of non-beneficial parts of the native structure
unlimited (source) material
cost (provided that a simple, large scale synthesis is possible)
stability/transport/storage

Synthetic compound vaccines ideally meet the requirements for synthetic "new generation" vaccines which may be summarized as follows [54,286]:

Safety

The costs of high liability make manufacturers devote strong efforts to establishing the complete innocuity of killed viral vaccines and evaluating the likelihood of genetic reversion of live, attenuated vaccines.

Large scale production/the cost factor

Large amounts of infectious material are needed for preparing any vaccine, requiring cumbersome safety precautions. Some infectious agents do not grow in culture or only in unacceptable systems that may present a danger to vaccine recipients. Synthetic source materials are cheap and available in abundance.

Antigenic variability of the pathogen

Agents that undergo antigenic variation are responsible for the most serious public health problems related to infectious diseases (e.g. HIV, malaria, influenza). This requires continuous development of new vaccines for which new rational and "synthetic" approaches (recombinant DNA technology, combinatorial chemistry) would facilitate changes to account for the genetic variation.

There are potential disadvantages, however, safety and costs. Synthetic vaccines might contain remnants of toxic chemicals. If the development of synthetic vaccines entails a complex, high cost technology, the cost factor may be incompatible with the potential market or competing pharmaceuticals.

Based on promising experiments in the early eighties, hopes were stimulated that synthetic peptide vaccines would soon be a reality. Major efforts were devoted to Foot-and-Mouth disease virus (FMDV), one of the simplest pathogens.

A synthetic peptide of FMDV was designed that efficiently induced antibodies which neutralized the virus *in vitro* and protected laboratory animals *in vivo*. Unfortunately, the synthetic peptide was never able to induce full protection in the natural hosts (bovines, swine, sheep and goats). Full protection is easily obtained using the classical FMDV vaccine based on whole inactivated virus.

Due to these disappointing results, interest in synthetic vaccines and the initial enthusiasm ignited by Merrifield's work about the inherent possibilities of solid phase peptide synthesis for vaccine development dwindled. The relationship between antigen and protection appeared to be far more mysterious than previously anticipated. Thus, at the end of the eighties, the general feeling was that effective synthetic vaccines were not a real option.

Then, a few years ago, the first synthetic peptide vaccine was developed that was able to induce full protection against parvoviruses in the natural host, dogs and minks [287]. This success paved the way to define more precisely the key players responsible for protection against this and other pathogens at the molecular level.

Heralds of feasible strategies in synthetic vaccine development were "second generation" vaccines. These link bacterial capsular polysaccharides to proteins, thereby improving their immunogenicity. Examples are protein conjugated vaccines against *Haemophilus influenzae* Type b (Hib vaccines) [288,289].

Our current understanding of immunological antigen presentation is rapidly increasing and it is clear that the initial drawbacks in peptide vaccine design were due to the incomplete knowledge of what really happens during antigen processing and presentation. As we learn how peptides are processed and what the fundamental requirements for antigenicity are, new peptide vaccines are coming in sight [60,71,72,290,291]. Besides increasing knowledge in immunology and physiology, technical advances such as combinatorial chemistry and automated high throughput techniques have practical consequences for peptide vaccine development.

An exciting approach is based on combinatorial peptide libraries mentioned above. Jung, Fleckenstein and co-workers synthesized a comprehensive library of 19^7 octapeptides. These 8-mers include the complete "universe" of (human) MHC I binding T cell epitopes [292,293]. As MHC I binding is a very stringent phenomenon [294], Jung and his colleagues could systematically catalogue peptide binding

specificity of MHC I and are now able to predict class I MHC binding motifs in proteins. Synthetic peptides representing viral CTL-epitopes have been shown to induce the same high-affinity CTLs (cytotoxic T-lymphocytes) as the infectious virus itself [295,296,296]. And selective (*in-vitro*) CTL-stimulation repeatedly demonstrated the potential to fight or control viral infections such as HIV [297,298].

As a consequence, computer-designed peptidic CTL vaccines are within reach: Take a virus, sequence it, predict the MHC I binding motifs from a couple of virus proteins, make peptides, vaccinate.

This near-future vision for synthetic peptide vaccines is exciting. However, CTL vaccines can only stimulate the cellular response and will probably work as therapeutic vaccines in viral infections only. In contrast, protective immunity requires the utilization of MHC II binding motifs and identification of antibody binding sites for a well targeted stimulation of the humoral immune response. MHC II binding motifs are much more degenerate than MHC I [6,281,282] and the structural biology of antibody-epitope interaction is complicated.

Nevertheless, the above strategy allows cytotoxic T cells to be deliberately stimulated to patrol the immune system for cells which harbor viruses. Clinical trials are under way for HBV and HIV [299]. Peptide vaccines are on the agenda again.